

Anti-oncogenic effects of RP10107, a novel and potent glutaminase inhibitor, in cancer cell lines

Srikant Viswanadha^{2*}, Prashant Bhavar¹, Gayatriswaroop Merikapudi², Babu Govindrajulu², Satyanarayana Eleswarapu², Sridhar Veeraraghavan² and Swaroop Vakkalanka¹

¹Rhizen Pharmaceuticals SA, La Chaux de Fonds, Switzerland, ²Incozen Therapeutics Private Limited, Hyderabad, India,

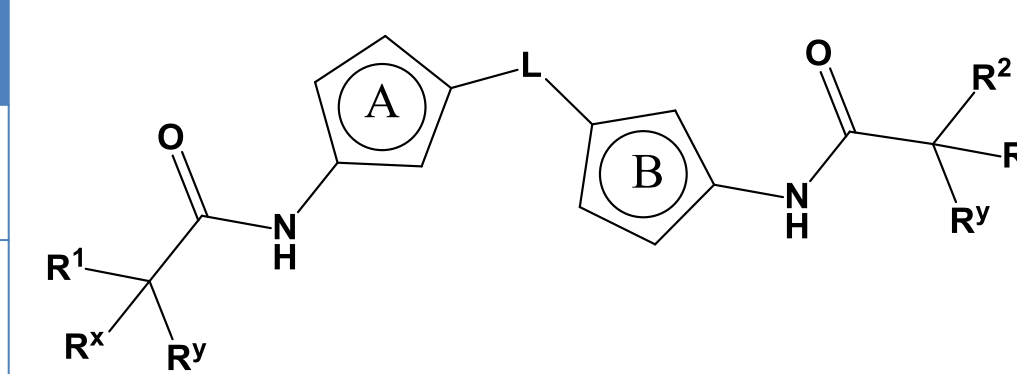


Introduction

Most normal cells use glucose as a fuel source wherein glucose is metabolized by glycolysis in a multi-step set of reactions resulting in the creation of pyruvate. Pyruvate enters the mitochondria where it is oxidized by the Krebs Cycle to generate ATP to meet the cell's energy demands. However, cancer cells or other highly proliferative cell types preferentially channel glucose towards lactate production even when oxygen is plentiful, a process termed "aerobic glycolysis" or the Warburg Effect. The entire metabolic machinery is therefore reprogrammed in cancer cells in order to compensate for the aforementioned changes. To help maintain a functioning citric acid cycle, cancer cells utilize glutamine via elevation of glutaminase activity thereby generating the necessary substrates required for eventual ATP synthesis and energy production. Targeting glutaminase therefore represents a potential therapeutic strategy to prevent malignant transformation of cells and combat cancer progression. Herein, we describe the biological and pharmacokinetic properties of RP10107, a novel small molecule glutaminase inhibitor, with scope to be further developed as a clinical candidate for solid tumors and hematological malignancies.

Enzyme & Cell-based activity

Glutaminase	Species	IC ₅₀ (nM)
GLS-1 (Kidney type)	Human	26.4
	Mouse	21.2
	Rat	18.2
GLS-2 (Liver type)	Mouse	



All variables are as defined in PCT/IB2015/050075

Table 1. Glutaminase inhibition by RP10107. IC₅₀ of RP10107 using recombinant human GLS-1 or mouse liver mitochondria derived GLS-2 was determined by measuring the conversion of glutamine to α-ketoglutarate fluorometrically. Activity of RP10107 against mouse or rat GLS-1 was determined colorimetrically using brain lysates in an ammonia release assay. **RP10107 demonstrated >350 selectivity over GLS-2**

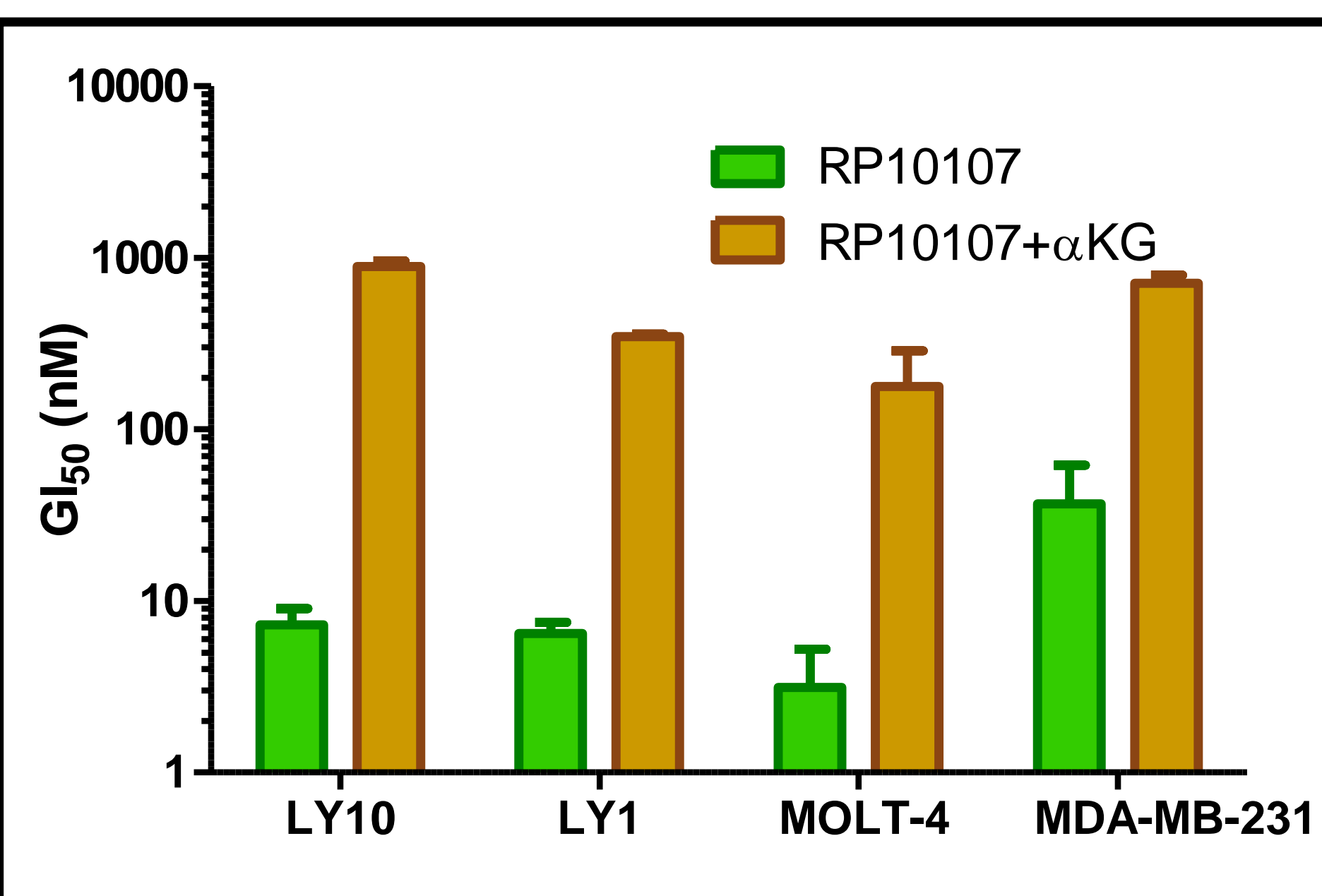


Figure 1. Addition of α-ketoglutarate (αKG) reverses the anti-proliferative effect of RP10107. Cell lines were plated in media at a pre-determined cell density in 96-well plates. Following overnight incubation, cells were treated with 100X concentration of RP10107 to bring the final concentration to 1X in total 150 μl volume (±1mM αKG). After 72 h, MTT was added and GI₅₀ was calculated using Graphpad prism. **Results demonstrated a several fold change in GI₅₀ of selected cell lines upon addition of αKG**

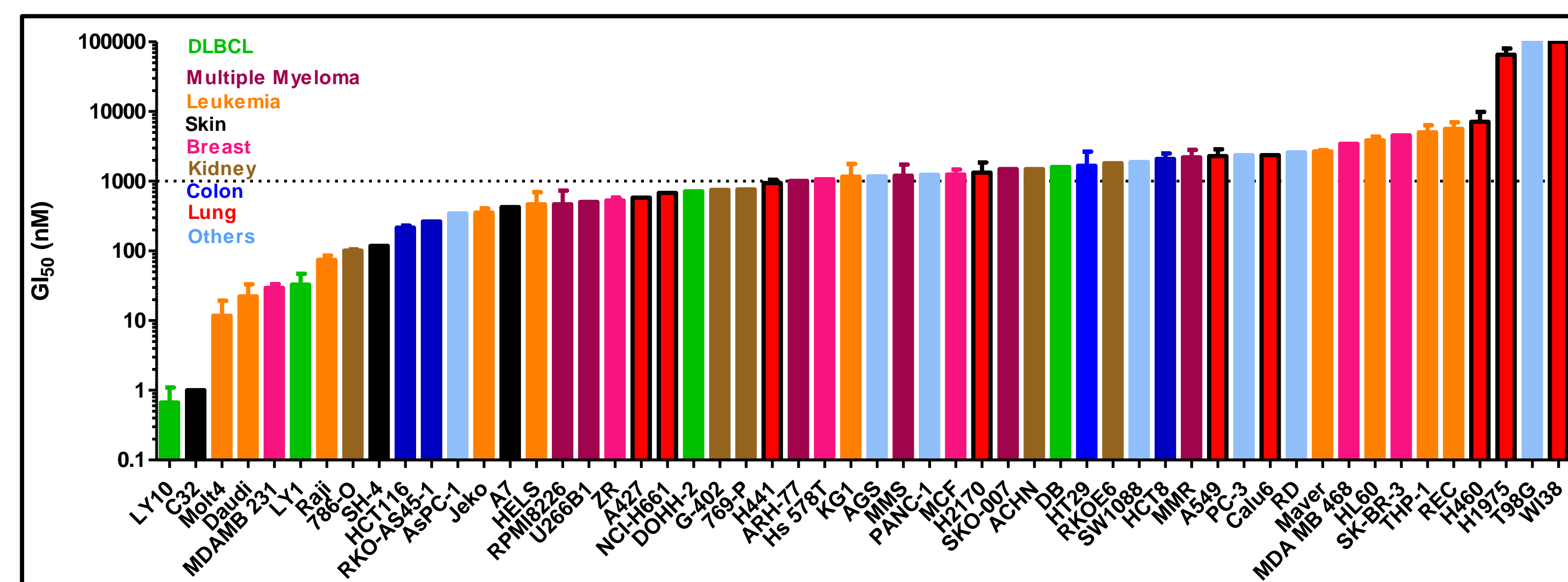


Figure 2. Anti-proliferative effect of RP10107 across cell lines. Cell lines were plated in media at a pre-determined cell density in 96-well plates. Following overnight incubation, cells were treated with 100X concentration of RP10107 to bring the final concentration to 1X in total 150 μl volume (±1mM αKG). After 72 h, MTT was added and GI₅₀ was calculated using Graphpad prism. **Majority of the cell lines tested were sensitive to RP10107 with GI₅₀ ranging between 1-1000 nM**

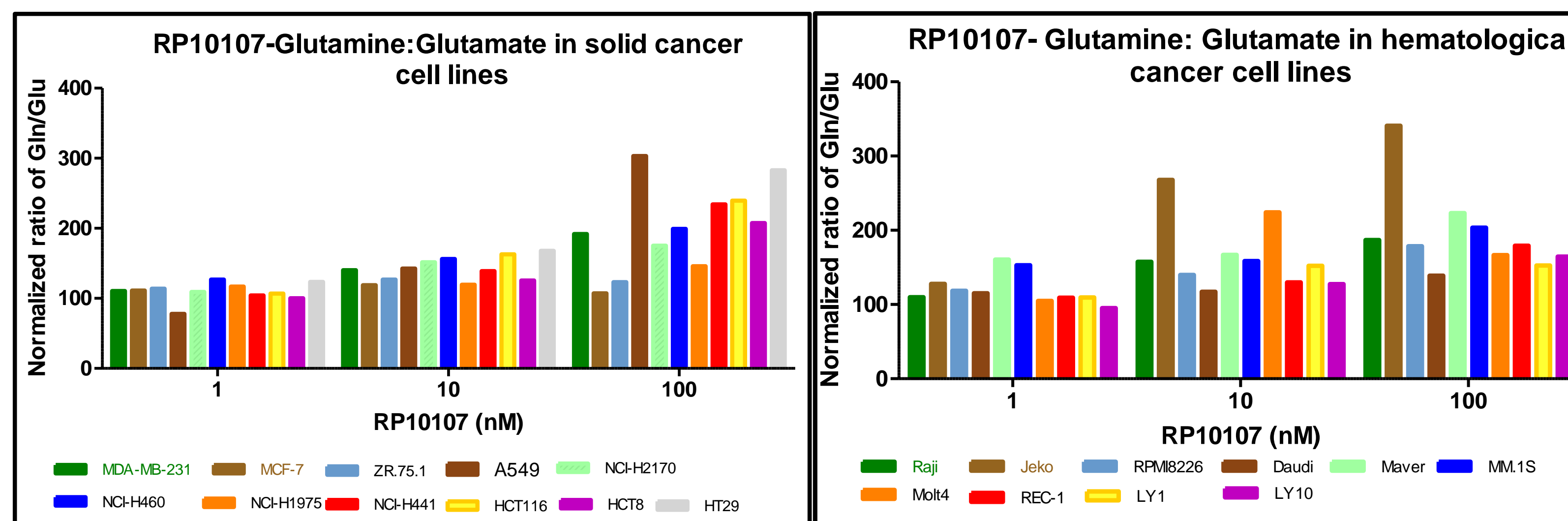


Figure 3. Glutamine to glutamate conversion in cancer cell lines. Cells were plated and incubated overnight in 24-well plates and treated with RP10107. Cells were incubated at 37 °C for 24-hours post treatment. Adherent cells were washed in the plate while suspension cells were collected and washed with PBS. Cells were lysed using 50% methanol in water incubated on ice for 30 min. Following centrifugation, supernatant was collected and glutamine and glutamate concentrations were determined on a LC-MS/MS. **Inhibition of glutaminase by RP10107 caused accumulation of glutamine within cells with a subsequent increase in the ratio of glutamine: glutamate.**

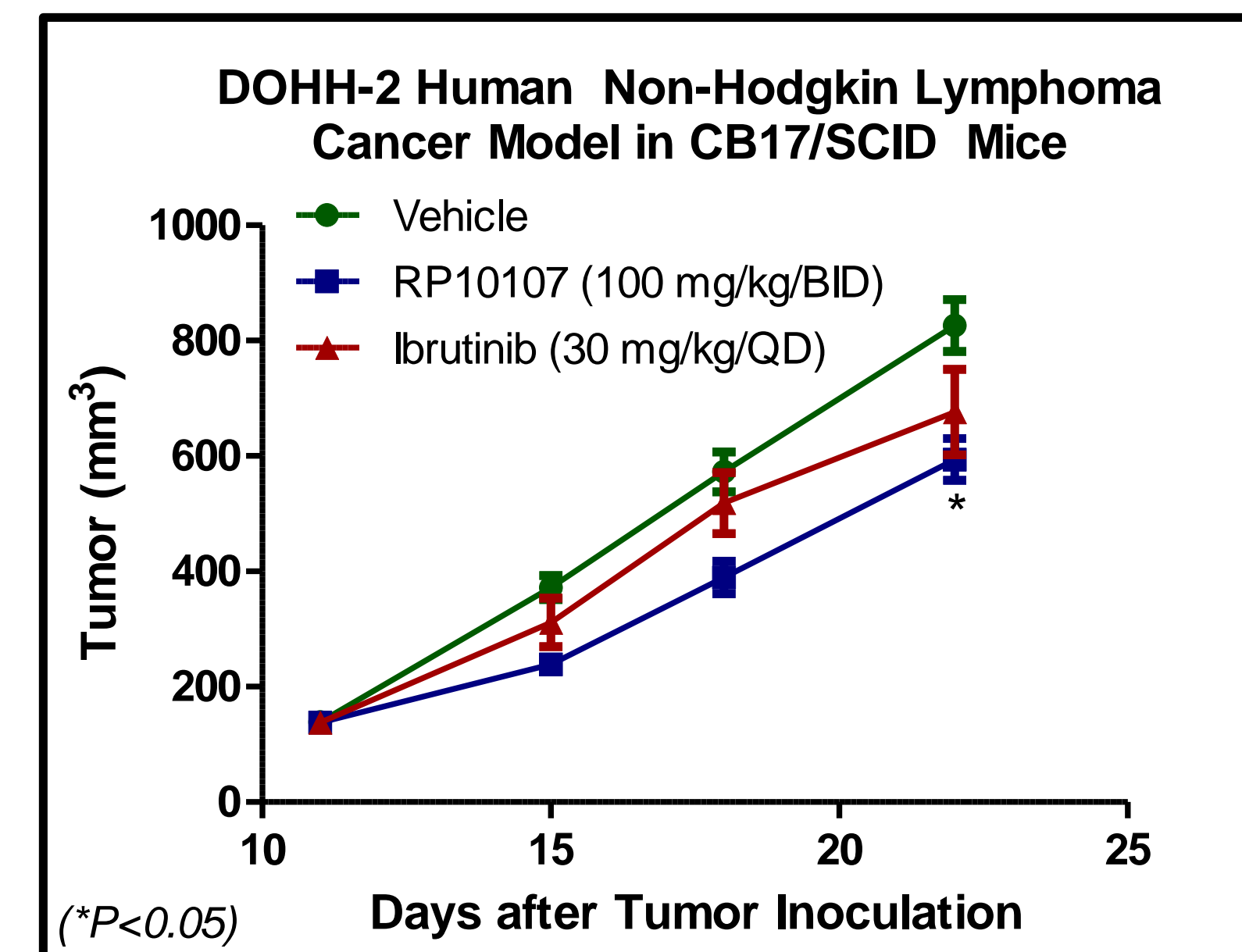


Figure 4. Efficacy in a subcutaneous DOHH-2 xenograft mouse model. CB17/SCID mice were inoculated subcutaneously at the right flank region with DOHH-2 tumor cells (5 x 10⁶) in 0.1 ml of PBS mixed with matrigel (1:1) for tumor development. Compound treatment was initiated when the mean tumor size reached approximately 125-150 mm³. **Data indicate a marked anti-tumor effect of RP10107 indicating its utility in DLBCL.**

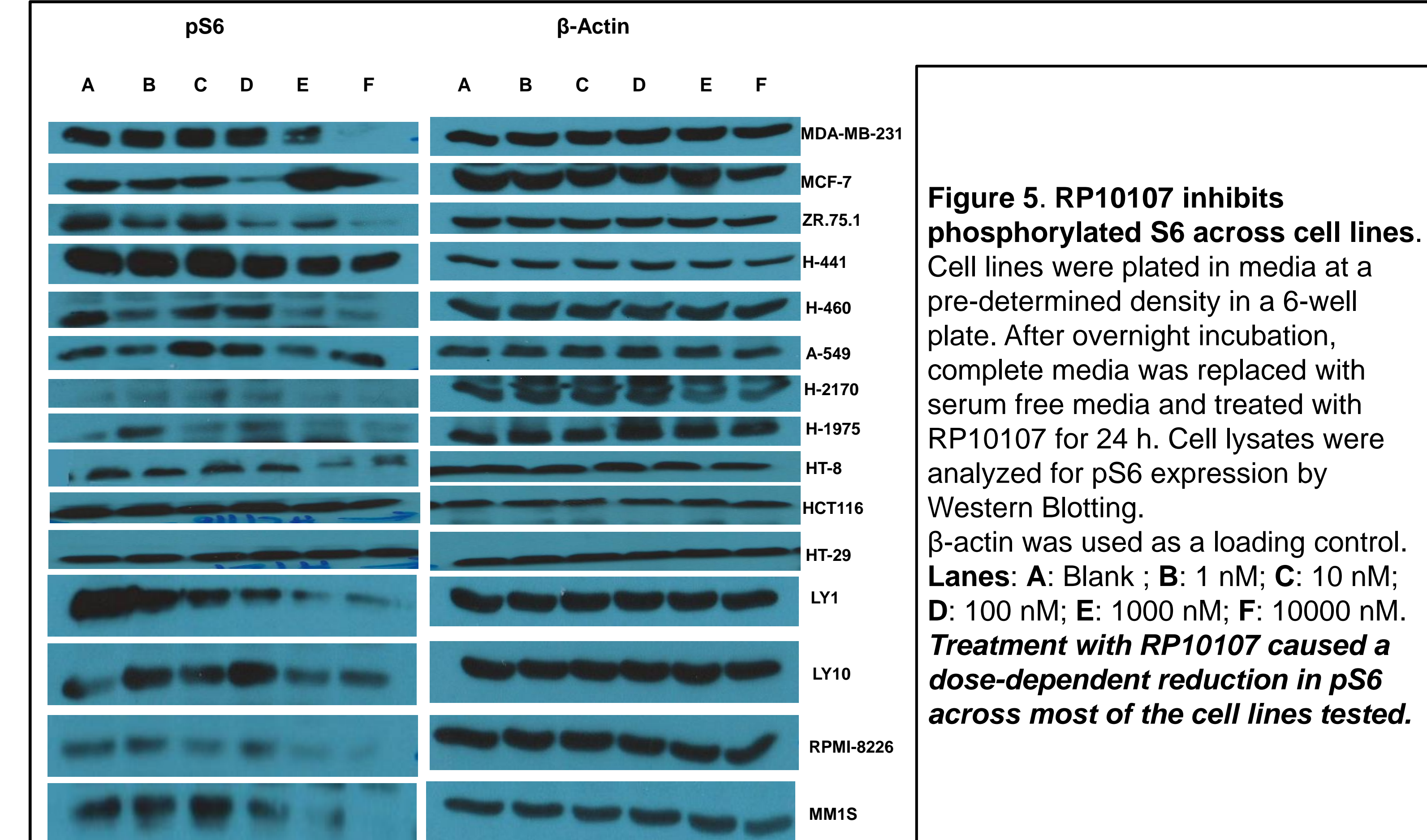


Figure 5. RP10107 inhibits phosphorylated S6 across cell lines. Cell lines were plated in media at a pre-determined density in a 6-well plate. After overnight incubation, complete media was replaced with serum free media and treated with RP10107 for 24 h. Cell lysates were analyzed for pS6 expression by Western blotting. β-actin was used as a loading control. **Lanes: A: Blank; B: 1 nM; C: 10 nM; D: 100 nM; E: 1000 nM; F: 10000 nM. Treatment with RP10107 caused a dose-dependent reduction in pS6 across most of the cell lines tested.**

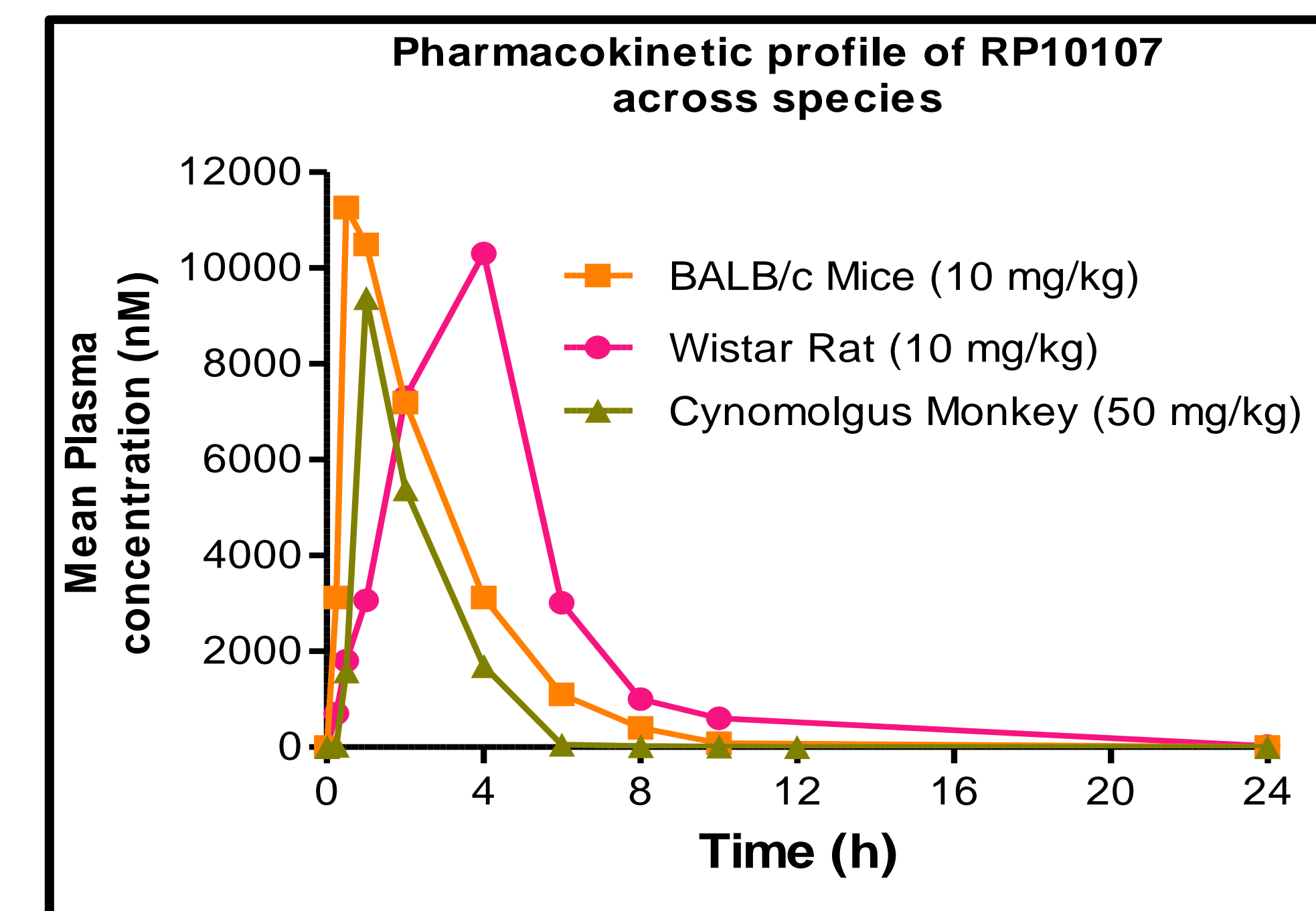


Figure 6. Single dose pharmacokinetic profile of RP10107 in mice, rat, and dog. Compound was administered orally as a suspension followed by blood collection across a 24-h period. Plasma was harvested and analyzed for RP10107 concentrations by LC-MS/MS. **RP10107 was rapidly absorbed reaching up to 10 μM concentrations at the doses tested**

SUMMARY & CONCLUSIONS

- RP10107 is a potent inhibitor of GLS-1 with several fold selectivity over the liver isoform
- Mechanism of action confirmed in several secondary assays by estimating glutamate formation as well as reversal of activity after addition of α-KG.
- Demonstrated activity in several cell lines representative of solid tumors and hematological malignancies
- Favorable pharmacokinetics with demonstrated efficacy in a DOHH-2 mouse xenograft model

